Displays 75 (2022) 102304

Contents lists available at ScienceDirect

Displays

journal homepage: www.elsevier.com/locate/displa

Photoluminescence properties of Eu^{3+}-doped Na_2CaSiO_4 phosphor prepared by wet-chemical synthesis route☆

Yatish R. Parauha [a,*], D.K. Halwar [b], S.J. Dhoble [b]

[a] Department of Physics, R.T.M. Nagpur University, Nagpur 440033, India
[b] Department of Electronics, M.S.G. College, Malegaon Camp-423105, India

ARTICLE INFO

Keywords:
Phosphor
Light-emitting diode (LED)
Photoluminescence (PL)
Wet chemical method

ABSTRACT

The present investigation focuses on the development of Eu^{3+} activated phosphors for near ultraviolet (NUV) excited light emitting diode (LED) applications. In this investigation, we have synthesized a series of Na_2CaSiO_4:Eu^{3+} phosphors via wet-chemical method and characteristic of synthesized phosphors have been analyzed by X-ray diffraction (XRD), Scanning electron microscopy (SEM), Thermo gravimetric analysis– Differential thermal analysis (TGA–DTA) and photoluminescence (PL) techniques. The recorded excitation band indicates a broad excitation band centered at 262 nm due to charge transfer (CT) band and sharp peaks at 395 nm and 466 nm due to $^7F_0 \rightarrow {}^5L_6$ and $^7F_0 \rightarrow {}^5D_2$ transition of Eu^{3+} ions. The highest excitation intensity was observed at 396 nm wavelength. Therefore under 396 nm excitation, the emission spectrum showed characteristics peaks located at 595 nm and 615 nm, which are attributed due to the $^5D_0 \rightarrow {}^7F_1$ and $^5D_0 \rightarrow {}^7F_2$ transition of Eu^{3+} ions. Emission spectra shows dominant emission peak at orange region around 595 nm due to the magnetic dipole transition of $^5D_0 \rightarrow {}^7F_1$. In addition, the effects of the Eu^{3+} ions on the emission intensity were investigated, it was found that the emission intensity increases as the concentration of Eu^{3+} ions increases up to 0.5 mol%. Thereafter, PL emission intensity was decreased due to concentration quenching. The CIE Chromaticity coordinate of the prepared phosphor was located in the orange region around (0.584, 0.421) with high color purity. As per the investigation of prepared Na_2CaSiO_4:Eu^{3+} phosphors, it was concluded that it is a promising candidate for lighting and display applications.

1. Introduction

In the past few decades, rare-earth activated phosphors have attracted great attention from research scholars and the scientific community, because of their wide applications, such as lighting, displays, lasers, solar cells, sensors, bio-imaging, fingerprint detection, photo-therapy, and plant growth, etc[1–10]. Already as a commercially applicable product, the developed inorganic phosphors play an important role in White LEDs (WLEDs) [11–13]. In the modern era, lighting devices consume a large amount of energy for low output voltages. WLEDs are the only lighting devices that provide high output. In the field of lighting, LEDs have attracted worldwide attention, mainly due to their advantages such as energy saving, eco-friendly features, fast switching, and lifetime, etc[11–14]. Currently, blue LED chips coated with $Y_3Al_5O_{12}$ (YAG):Ce^{3+} yellow emitting phosphors are used in the most commercial WLEDs [15]. However, this approach is facing several problems such as low color rendering index (CRI < 70), high correlated color temperature (CCT > 7000 K), and lack of red emission in the luminescence spectra [15–18]. One of the simplest and most researched ways to overcome these anomalies of YAG:Ce^{3+} and to obtain white light is the development of orange-red phosphors. So, research community trying to development of highly efficient novel red emitting LED phosphors.

In the current status, a number of research papers are published for the development of orange red emitting phosphors and trying to improve the luminescence properties of the existing phosphors. Especially, Eu^{3+} activated phosphors have been investigated in detailed. As per the literature, Eu^{3+} is interesting lanthanide ion because it's have potential for lighting and display devices. Generally, Eu^{3+} activated phosphors exhibits strong sharp emission peaks in the orange region around 593 nm and the red region around 615 nm due to the $^5D_0 \rightarrow {}^7F_1$ and $^5D_0 \rightarrow {}^7F_2$ transition of Eu^{3+} ions [8,10,19]. Yongbin Hua et al [16]

☆ This paper was recommended for publication by Prof G Guangtao Zhai.

* Corresponding author.
E-mail address: yatishparauha15@gmail.com (Y.R. Parauha).

https://doi.org/10.1016/j.displa.2022.102304
Received 22 February 2022; Received in revised form 17 August 2022; Accepted 19 September 2022
Available online 24 September 2022

investigated Eu^{3+} activated Sr_3MoO_6 red emitting phosphors by solid state reaction method. Under these UV and blue excitations, the synthesized phosphors show superior luminescence properties and suitability for the WLEDs and flexible display film. S. Wang et al [20] reported red emitting $Ba_3Lu_4O_9:Eu^{3+}$ phosphors for warm white light emitting diodes (WLEDs). Peng Du et al [21] reported red emitting Eu^{3+} activated $NaBiF_4$ phosphors that exhibit strong red emission due to the dipole–dipole interaction with 73.1 % internal quantum efficiency. X. Huang et al [22] investigated $Na_2Gd(PO_4)(MoO_4)$ phosphors, which are synthesized via solid-state reaction method. In his investigation, the authors reported that the synthesized phosphors exhibit strong red emission under NUV excitation around 395 nm. T. Sakthivel et al [23] reported Eu^{3+} activated $Na_2Y_2B_2O_7$ phosphors and reported red emission under NUV excitation with 36.6 % internal quantum efficiency.

Generally, it is well known that the luminescence properties of rare earth doped phosphors are strongly depending on the host materials. Therefore, the selection of proper host materials is an important task for the development of rare earth activated phosphors for WLEDs. Up to till date, various inorganic host materials were synthesized such as such as fluoride, molybdate, germanate, silicates, tungstate, etc. matrix. Nowadays, A_2(A = Li, Na, K)M(M = Ca, Sr, Ba, Mg)SiO_4 systems have been extensively investigated for WLEDs by several scholars and scientists, because of their excellent thermal and hydrolytic stabilities that meet the requirements for efficient host materials[24,25]. Therefore, we have chosen the silicate based material as the host and doped Eu^{3+} ions. In the present investigation, Eu^{3+} activated Na_2CaSiO_4 phosphors were synthesized by wet chemical method and their luminescence properties were analyzed. In the past, Huang et al [26] investigated Eu^{3+} and Dy^{3+} doped and co-doped Na_2CaSiO_4 phosphors by sol–gel method and their photoluminescence properties studied systematically. Xie et al [27] reported deep red-emitting $Na_2CaSiO_4:Eu^{3+}$ phosphors by solid state reaction method. Shi et al [28] also reported $Na_2CaSiO_4:Eu^{3+}$ phosphors by solid state reaction method. In the both investigation, photoluminescence properties investigated and red color emission observed, suggested that $Na_2CaSiO_4:Eu^{3+}$ phosphors are potential candidate for light-emitting diodes. To the best of our knowledge, the $Na_2CaSiO_4:Eu^{3+}$ phosphor was first time reported by wet chemical method. The synthesized phosphors were characterized by XRD, SEM, TGA-DTA, and PL technique. Our results revealed that the synthesized phosphors have high possibilities and that it can be useful for lighting and display applications.

2. Experimental details

2.1. Material preparation

In this investigation, a series of Na_2CaSiO_4:x.mol%Eu^{3+} (x = 0, 0.1, 0.2, 0.5, 0.7, 1.0 mol %) phosphors were prepared by wet chemical method. Sodium nitrate [$NaNO_3$], calcium nitrate [$Ca(NO_3)_2{\cdot}4H_2O$], silicon dioxide (SiO_2), europium oxide [Eu_2O_3] were used as raw materials in this synthesis. All these raw materials were purchased from Loba chemie with A.R. grade and 98–99.99 % purity. In this synthesis, all raw materials were weighed according to the composition, then transferred to a glass beaker and dissolved with double distilled water. Here, Eu is available as an oxide form, so we convert it to nitrate form by dissolving stoichiometric amounts of europium ions in a concentrated HNO_3. The mixed solution with distilled water was stirred using a magnetic stirrer at 80 °C. The precipitate product was filtered and washed with acetone for several times and then dried in an oven for overnight. The obtained powder was crushed with mortar and pestle to a fine powder then placed in a crucible and annealed for 5 hrs in a furnace at 800 °C. Thereafter, the obtained powder was used for further characterization.

2.2. Characterization techniques

In the current investigation, XRD pattern of the synthesized material was analyzed by Rigaku miniflex d 600 X-ray diffractometer in the range of 10° to 70° with 0.02°/*sec* scanning rate. The size of the particle and morphological behavior were analyzed by JSM-6360LV scanning electron microscope (SEM) instrument (JEOL, USA). Shimadzu DTG-60 simultaneous DTATG apparatus was used for thermal stability analysis of the synthesized material. The Shimadzu RF5301PC Spectrofluorophotometer was used for the analysis of PL excitation and emission spectra. The photometric properties like CIE coordinates and color purity have been analyzed by the OSRAM SYLVANIA color calculator.

3. Results and discussion

3.1. XRD measurement

Fig. 1 shows the XRD pattern of our synthesized undoped and doped Na_2CaSiO_4 phosphor and the measured pattern is compared with the standard ICSD data file no. 98–002-4235. The XRD pattern clearly demonstrated that all diffraction peaks of the synthesized sample was matched well with the standard data and there were no additional peaks were found that confirmed the synthesized material was successfully prepared. The XRD pattern of the Eu^{3+} doped Na_2CaSiO_4 phosphor was similar to that of the undoped phosphor implying that the doping of Eu^{3+} ions does not change the crystal structure of the Na_2CaSiO_4 host. It is also clear from Fig. 1 that the diffraction peaks are sharp and intense, which is suggested that the prepared phosphor was crystalline in nature and homogeneous form. The Na_2CaSiO_4 phosphor has a cubic structure with Fm3m (225) space group. From the literature, it was found that ionic radii of Ca^{2+} and Eu^{3+} is 1.26 Å (CN = 8), 1.20 Å (CN = 8), respectively. Therefore, it is assumed that Eu^{3+} will enter in the place of Ca^{2+} ions. Furthermore, to better understand the dopant Eu^{3+} ions occupying Ca^{2+} sites in the Na_2CaSiO_4 host lattice, the radius percentage difference (D_r) between substituted ions and active ions should be obtained, which can be defined by the following expression [16]:

$$D_r = \frac{R_1(CN) - R_2(CN)}{R_1(CN)} \times 100\% \quad (1)$$

Here, R_1 (CN) is radii of substituted (Ca^{2+}) and R_2 (CN) is radii of activated Eu^{3+}. If the D_r is smaller than 30 %, it is much easy to come into being a new solid-solution. With the help of Eq. (1), the value of D_r was calculated to be 4.76 % when CN = 8, suggesting that the Eu^{3+} could well substitute Ca^{2+} ion sites in Na_2CaSiO_4 host lattices.

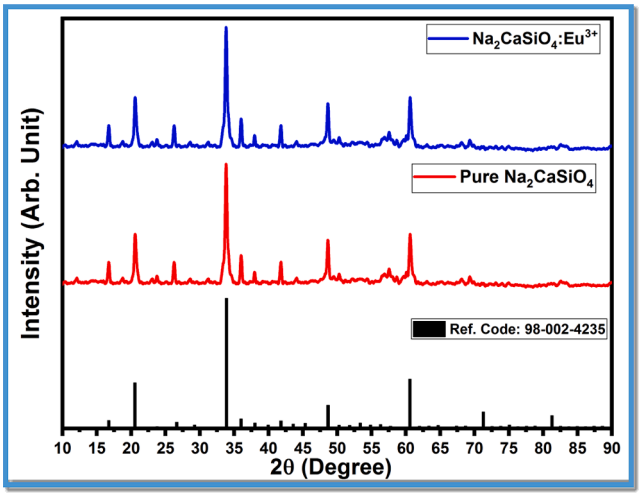

Fig. 1. XRD Pattern of prepared Na_2CaSiO_4 phosphor and compared with ICSD. 98–002-4235.

3.2. Morphological behaviour

Fig. 2 revealed SEM micrographs of prepared Na_2CaSiO_4 phosphor. It was clear from the obtained SEM images that the particles are irregular in shape and agglomeration can easily see in the images, this may be possibly due to high temperature annealing. The average particle size of the prepared sample is found in the micrometers dimension. According to the literature, the morphological behavior of the prepared sample affects the luminescence properties. The literature suggests that the submicron size particle enhances the luminescence properties of the prepared sample [29–31]. The occurrence of submicron size particle along with better crystallinity is suitable for efficient white LEDs.

3.3. Thermal behaviour

The thermal stability of the prepared sample has been analyzed by TG-DTA technique. Fig. 3 shows TG-DTA curve of the prepared Na_2CaSiO_4 phosphor, which has been measured from room temperature to 800 °C. The DTA curve shows two endothermic bands around 100 °C and 180 °C, which may be possibly due to the evaporation of moisture and removal of gases. The TGA curve shows a total weight loss around 8–9 % that confirmed that the synthesized phosphors has excellent thermal stability.

3.4. Photoluminescence (PL) properties

The PL excitation spectrum of the synthesized Na_2CaSiO_4: 0.5 mol% Eu^{3+} phosphor has been monitored under 595 nm emission wavelength in the range of 220 nm to 500 nm, as shown in Fig. 4. The monitored excitation band exhibits a broad excitation band centered at 262 nm, which is known as the charge transfer (CT) band attributed due to the charge transition from oxygen 2p orbital (O^{2-}) to the vacant europium 4f orbital (Eu^{3+}) ions. Apart from this, several sharp excitation bands exhibit around 320 nm, 363 nm, 385 nm, 395 nm, 466 nm. These excitation band corresponded due to $^7F_0 \rightarrow {}^5H_6$, $^7F_0 \rightarrow {}^5D_4$, $^5F_0 \rightarrow {}^5G_3$, $^7F_0 \rightarrow {}^5L_6$, $^7F_0 \rightarrow {}^5D_2$ transitions of Eu^{3+} ions, respectively [16,22]. The measured excitation spectrum shows the most intense excitation band around 395 nm, which is matched well with the excitation of the commercial NUV LED chips.

Under 395 nm excitation, PL emission spectra have been recorded for different concentration of Eu^{3+} ions in the range of 540 nm to 660 nm, as shown in Fig. 5. The showed emission spectrum exhibits orange and red emission bands around 588 nm, 595 nm, and 615 nm, respectively. The orange emission band splits into two emission bands, which may be possibly due to the crystal field effect. According to the crystal field effect, one transition can be splitted into one or more transitions. The observed orange emission bands (588 nm and 595 nm) are attributed to the $^5D_0 \rightarrow {}^7F_1$ and red emission band is corresponded to the $^5D_0 \rightarrow {}^7F_2$ transitions of Eu^{3+} ions. According to the literature, $^5D_0 \rightarrow {}^7F_1$ transition is known as magnetic dipole (MD) transition and $^5D_0 \rightarrow {}^7F_2$ transition is known as electric dipole (ED) transition. According to previous literature, the $^5D_0 \rightarrow {}^7F_1$ (MD) transition is independent of the coordination

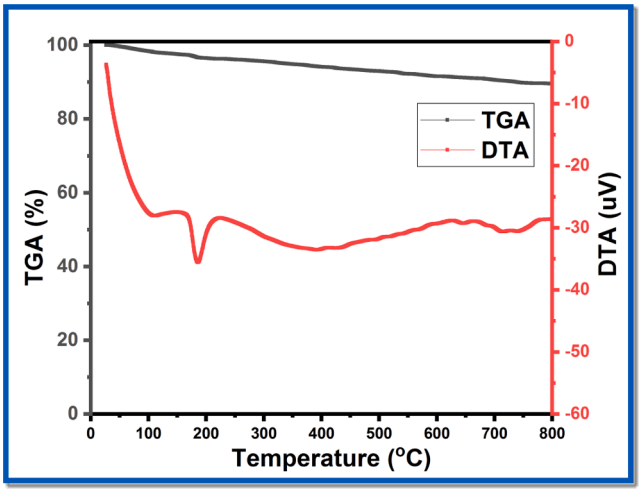

Fig. 3. TG-DTA curve of prepared Na_2CaSiO_4 phosphor.

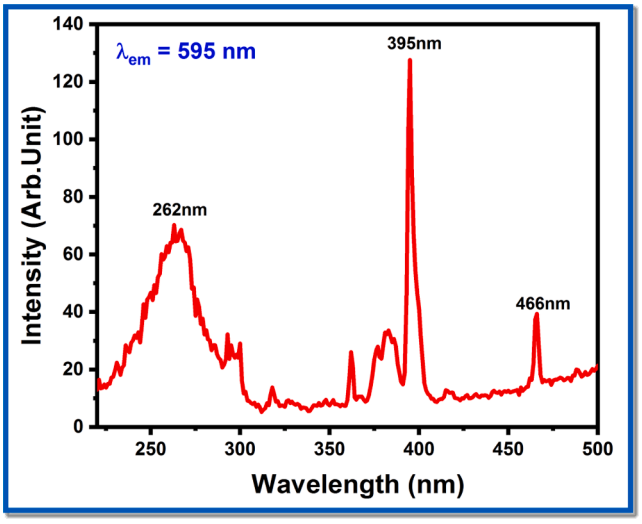

Fig. 4. PL Excitation spectrum of Na_2CaSiO_4:0.5 mol% Eu^{3+} phosphor monitored at 595 nm emission.

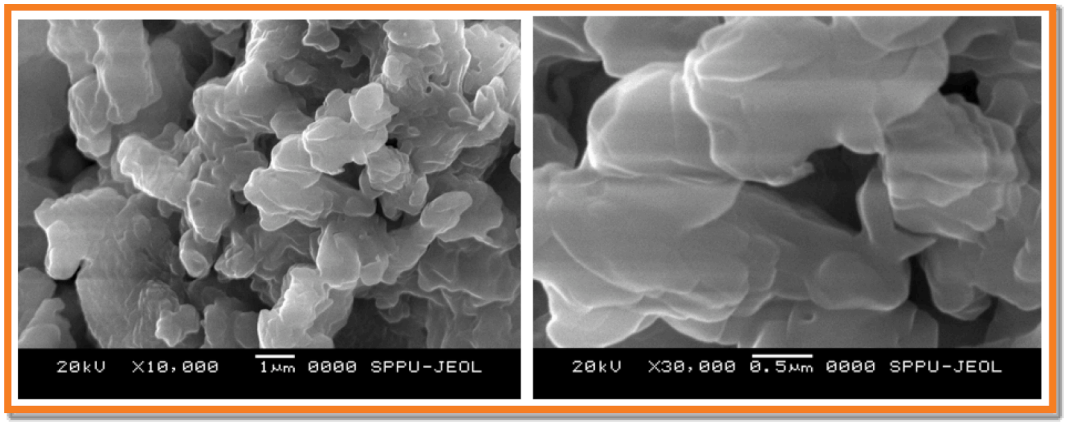

Fig. 2. SEM images of prepared Na_2CaSiO_4 phosphor.

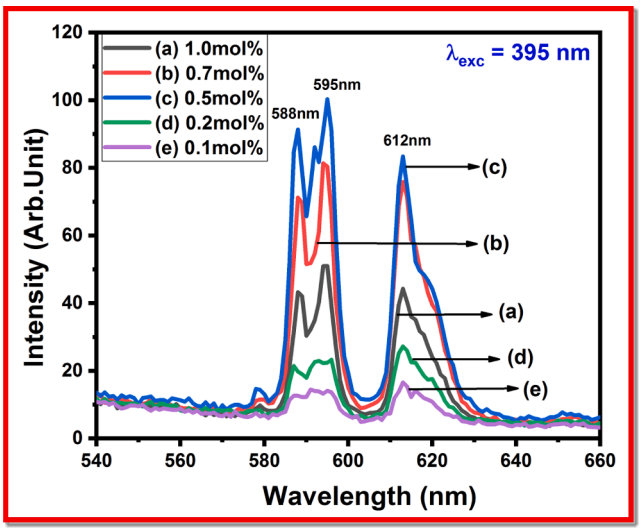

Fig. 5. PL emission spectrum of $Na_2Ca_{(1-x)}SiO_4$. × mol% Eu^{3+} phosphors (x = 0.1, 0.2, 0.5, 0.7, 1.0) mol% under 395 nm excitation.

surroundings of the host lattice, whereas the $^5D_0 \rightarrow {}^7F_2$ (ED) transition is highly dependent on the surrounding chemical environment of the dopant (Eu^{3+}). Emission spectra clearly depicted that MD ($^5D_0 \rightarrow {}^7F_1$) transition is dominant than ED transition, therefore previous studies suggested that Eu^{3+} ions occupy low symmetry sites with no inversion center [32,33]. The recorded emission spectrum show variation in emission intensity with variation in concentration of Eu^{3+} ions. The structure of the emission bands are similar for each concentration. Fig. 6 shows variation in emission intensity with variation of Eu^{3+} concentrations, which demonstrated the emission intensity increases up to 0.5 mol%, thereafter the emission intensity decreased due to concentration quenching. The reason behind concentration quenching is already explained in the various research papers [8,19,29,33].

The concentration quenching is strongly correlated with the critical distance (R_c) between the Eu^{3+} ions. According to the proposed model of Blasse's theory, the critical distance (R_c) between Eu^{3+} ions can be calculated using following formula [16,22]:

$$R_c = 2\left(\frac{3V}{4\pi X_c N}\right)^{\frac{1}{3}} \quad (2)$$

Where V = volume of a unit cell, X_c = critical concentration of Eu^{3+} ions, and N = number of Eu^{3+} sites in the unit cell. In the present investigation, V = 418.5 $Å^3$, N = 4 and X_c = 0.5. By using equation (2), the calculated value of R_c is around 11.69 Å. Previous studies suggested that if R_c < 5 Å then exchange interaction is responsible for concentration quenching. But if,R_c > 5 Å, then electric multipolar-multipolar interaction is responsible for concentration quenching [34,35]. In the current investigation, we found that the value of critical distance (R_c) is>5 Å, therefore the electric multipolar-multipolar interaction is responsible for concentration quenching in Eu^{3+} doped Na_2CaSiO_4 phosphor.

The strengths of multipolar-multipolar interaction were calculated using Dexter theory. According to Dexter theory, a relation between the concentration of dopants and their respective luminescence emission intensity was established, as given below in equation (3):

$$\frac{I}{x} = k[1 + \beta.x^{\frac{\theta}{3}}]^{-1} \quad (3)$$

Here, Where × = concentration of dopant, k and β is the constant, I = luminescence intensity, θ = strength of multipolar interaction. Literature suggested that the value of θ varies, indicating different types of interactions. Value of θ = 6, 8, 10 indicating dipole–dipole (d-d) interaction, dipole-quadrupole (d-q) interaction, quadrupole–quadrupole (q-q) interaction, respectively [36,37]. Fig. 7 demonstrates the plot of log (I/x) as a function of log (x) in Na_2CaSiO_4:Eu^{3+} phosphor. From the linear fitting of the experimental data, we have found negative slope value (-θ/3). The obtained value of θ is around to 6, therefore it was concluded that the dipole–dipole (d-d) interaction is responsible for the concentration quenching. Fig. 8 shows energy level diagram of Na_2CaSiO_4:Eu^{3+} phosphor.

3.5. Photometric characterization

The CIE chromaticity color coordinates of the synthesized samples was calculated using PL emission intensity and OSRAM SILVANIA color calculator 1931. Fig. 9 represents CIE chromaticity diagram of Na_2CaSiO_4:0.5 mol%Eu^{3+} phosphor. On the base of the PL emission spectrum, the chromaticity coordinate of the optimal doping concentration was calculated to be (0.584, 0.421) under 395 nm excitation wavelength. The plotted CIE chromaticity diagram shows the coordinate located in the orange-red region. The synthesized powder emitted red glow under UV light as shown in Fig. 10, implying that the Na_2CaSiO_4:0.5 mol% Eu^{3+} phosphor is a potential candidate to make WLEDs as a kind of red-emitting phosphors.

The color purity of the dominant emission color of Na_2CaSiO_4:0.5

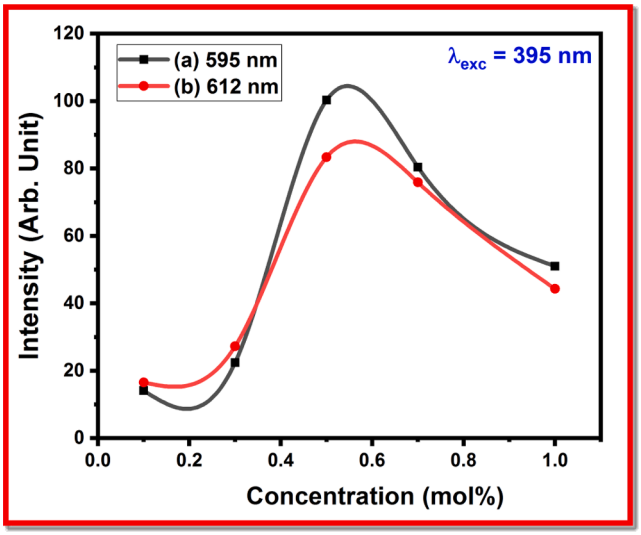

Fig. 6. Variation in emission intensity with variation of Eu^{3+} concentrations.

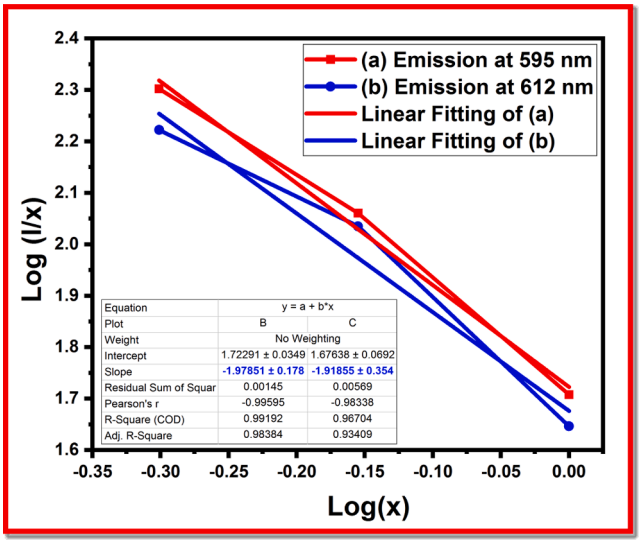

Fig. 7. Plot of log (I/x) as a function of log (x) in Na_2CaSiO_4:Eu^{3+} phosphor.

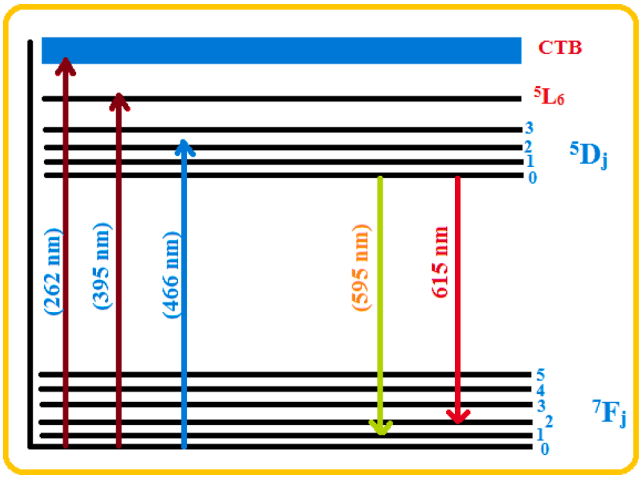

Fig. 8. Energy level diagram of $Na_2CaSiO_4:Eu^{3+}$ phosphor.

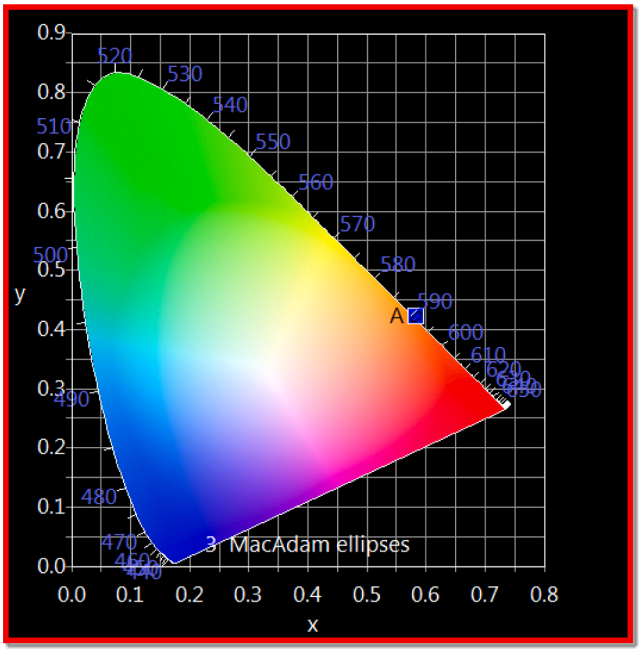

Fig. 9. CIE Chromaticity coordinate of Na_2CaSiO_4:0.5 mol%Eu^{3+} phosphor.

mol%Eu^{3+} phosphor were analyzed by using following equation [38]:

$$\textbf{4. Color purity} = \frac{\sqrt{(x-x_i)^2+(y-y_i)^2}}{\sqrt{(x_d-x_i)^2+(y_d-y_i)^2}} \times 100\% \cdots\cdots \quad (4)$$

Where (x, y) = CIE coordinate of phosphor, (x_i, y_i) = CIE coordinate of white illumination, (x_d, y_d) = CIE coordinate of dominated wavelength. In this investigation, (x = 0.584, y = 0.421), (x_i = 0.310, y_i = 0.316) and (x_d = 0.573, y_d = 0.416). Therefore, calculated color purity of synthesized Na_2CaSiO_4:0.5 mol%Eu^{3+} phosphor was around 95.65 %. The obtained result of Na_2CaSiO_4:0.5 mol%Eu^{3+} phosphor have high color purity for promising applications in WLEDs under NUV excitation.

5. Conclusion

In this investigation, we aimed to synthesis of $Na_2CaSiO_4:Eu^{3+}$ phosphors and investigate their luminescence properties. The different concentration of Eu^{3+} doped Na_2CaSiO_4 phosphors have been successfully prepared by wet chemical method and their PL excitation and emission properties have been reported. In addition, the phase purity, morphological behavior, and thermal stability of the prepared phosphors have been also reported in this investigation. The PL excitation spectrum shows excitation bands around 262 nm (CT band), 395 nm, and 466 nm. The 395 nm excitation band is the most intense excitation band and it matches well with the NUV excitation of the LED chip. Therefore, 395 nm excitation has selected for the emission spectrum measurement. The emission spectra of different concentration of Eu^{3+} activated Na_2CaSiO_4 phosphors has been exhibiting a strong orange and red emission band due to the $^5D_0 \rightarrow {}^7F_1$ and $^5D_0 \rightarrow {}^7F_2$ transition of Eu^{3+} ions. From the Dexter proposed model, it is clear that concentration quenching was observed due to dipole–dipole interaction. The CIE chromaticity coordinate of Na_2CaSiO_4:0.5 mol%Eu^{3+} phosphor was found around orange-red region with high color purity. The entire investigation and their output suggested that as synthesized Eu^{3+} doped Na_2CaSiO_4 phosphors have potential for lighting and display applications.

CRediT authorship contribution statement

Yatish R. Parauha: Methodology, Conceptualization, Investigation, Writing – original draft. **D.K. Halwar: . S.J. Dhoble:** Supervision, Writing – review & editing.

Declaration of Competing Interest

The authors declare that they have no known competing financial interests or personal relationships that could have appeared to influence the work reported in this paper.

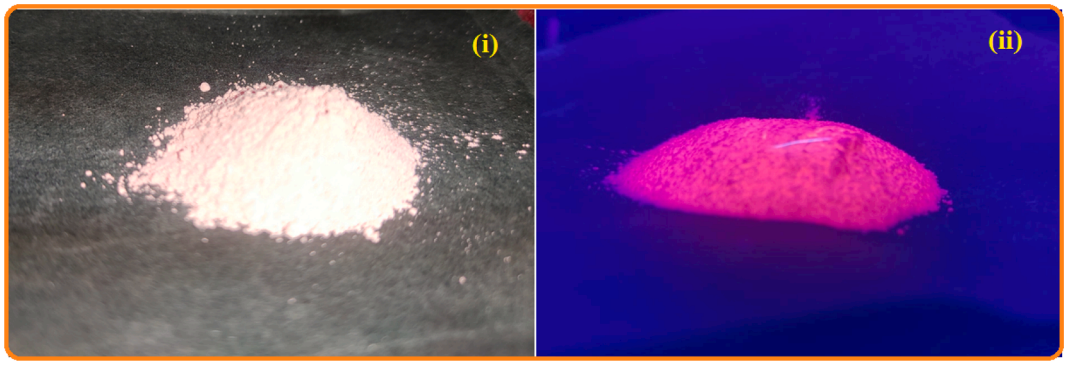

Fig. 10. Digital Photograph of synthesized Na_2CaSiO_4:0.5 mol%Eu^{3+} phosphor under (i) Normal light (Day light) (ii) UV light.

Data availability

Data will be made available on request.

Acknowledgement

One of the authors, Yatish R. Parauha, is thankful to Department of Science and Technology(DST), India for financial support through INSPIRE fellowship (INSPIRE Code – IF180284).

References

[1] Y. Wu, Y. Zhuang, Y. Lv, K. Ruan, R.J. Xie, A high-performance non-rare-earth deep-red-emitting $Ca_{14-x}Sr_xZn_6Al_{10}O_{35}:Mn^{4+}$ phosphor for high-power plant growth LEDs, J. Alloys Compd. 781 (2019) 702–709, https://doi.org/10.1016/j.jallcom.2018.12.056.

[2] S. Tamboli, G.B. Nair, S.J. Dhoble, D.K. Burghate, Energy transfer from Pr^{3+} to Gd^{3+} ions in BaB_8O_{13} phosphor for phototherapy lamps, Phys. B Condens. Matter. 535 (2018) 232–236, https://doi.org/10.1016/j.physb.2017.07.042.

[3] K.N. Kumar, L. Vijayalakshmi, P. Hwang, A.D. Wadhwani, J. Choi, Bright red-luminescence of Eu^{3+} ion-activated $La_{10}W_{22}O_{81}$ microphosphors for noncytotoxic latent fingerprint imaging, J. Alloys Compd. 840 (2020), 155589, https://doi.org/10.1016/j.jallcom.2020.155589.

[4] G. Ajithkumar, B. Yoo, D.E. Goral, P.J. Hornsby, A.L. Lin, U. Ladiwala, V.P. Dravid, D.K. Sardar, Multimodal bioimaging using a rare earth doped Gd_2O_2S:Yb/Er phosphor with upconversion luminescence and magnetic resonance properties, J. Mater. Chem. B. 1 (2013) 1561–1572, https://doi.org/10.1039/c3tb00551h.

[5] C. Gandate, Y.R. Parauha, S.G.M. Mushtaque, S.J. Dhoble, Current progress and comparative study of performance of the energy saving lighting devices: a review, J. Phys. Conf. Ser. 1913 (1) (2021) 012018, https://doi.org/10.1088/1742-6596/1913/1/012018.

[6] S. Khan, Y.R. Parauha, D.K. Halwar, S.J. Dhoble, Rare Earth (RE) doped color tunable phosphors for white light emitting diodes, J. Phys. Conf. Ser. 1913 (2021), 012017, https://doi.org/10.1088/1742-6596/1913/1/012017.

[7] R. Rajeswari, N. Islavath, M. Raghavender, L. Giribabu, Recent Progress and Emerging Applications of Rare Earth Doped Phosphor Materials for Dye-Sensitized and Perovskite Solar Cells: A Review, Chem. Rec. 20 (2) (2020) 65–88, https://doi.org/10.1002/tcr.201900008.

[8] S.R. Bargat, Y.R. Parauha, G.C. Mishra, S.J. Dhoble, Combustion synthesis and spectroscopic investigation of $CaNa_2(SO_4)_2:Eu^{3+}$ phosphor, J. Mol. Struct. 1221 (2020) 128838, https://doi.org/10.1016/j.molstruc.2020.128838.

[9] Y.R. Parauha, S.J. Dhoble, Thermoluminescence study and evaluation of trapping parameter of rare earth activated $Ca_3Al_2O_6$: RE (RE = Eu^{2+}, C^{e3}+) phosphors, J. Mol. Struct. 1211 (2020), 127993, https://doi.org/10.1016/j.molstruc.2020.127993.

[10] Y.R. Parauha, R.S. Yadav, S.J. Dhoble, Enhanced photoluminescence via doping of phosphate, sulphate and vanadate ions in Eu^{3+} doped $La_2(MoO_4)_3$ downconversion phosphors for white LEDs, Opt. Laser Technol. 124 (2020), https://doi.org/10.1016/j.optlastec.2019.105974.

[11] L. Li, W. Chang, W. Chen, Z. Feng, C. Zhao, P. Jiang, Y. Wang, X. Zhou, A. Suchocki, Double perovskite $LiLaMgWO_6:Eu^{3+}$ novel red-emitting phosphors for solid sate lighting: Synthesis, structure and photoluminescent properties, Ceram. Int. 43 (2017) 2720–2729, https://doi.org/10.1016/j.ceramint.2016.11.093.

[12] X. Huang, H. Guo, Finding a novel highly efficient Mn^{4+}-activated $Ca_3La_2W_2O_{12}$ far-red emitting phosphor with excellent responsiveness to phytochrome PFR: Towards indoor plant cultivation application, Dye. Pigment. 152 (2018) 36–42, https://doi.org/10.1016/j.dyepig.2018.01.022.

[13] D. Chen, Y. Zhou, J. Zhong, A review on Mn^{4+} activators in solids for warm white light-emitting diodes, RSC Adv. 6 (89) (2016) 86285–86296.

[14] C.M. Mehare, Y.R. Parauha, N.S. Dhoble, C. Ghanty, S.J. Dhoble, Synthesis of novel Eu^{2+} activated $K_3Ca_2(SO_4)_3F$ down-conversion phosphor for near UV excited white light emitting diode, J. Mol. Struct. 1212 (2020), 127957, https://doi.org/10.1016/j.molstruc.2020.127957.

[15] S. Wang, Q. Sun, B. Devakumar, J. Liang, L. Sun, X. Huang, Novel highly efficient and thermally stable $Ca_2GdTaO_6:Eu^{3+}$ red-emitting phosphors with high color purity for UV/blue-excited WLEDs, J. Alloys Compd. 804 (2019) 93–99, https://doi.org/10.1016/j.jallcom.2019.06.388.

[16] Y. Hua, S.K. Hussain, J.S. Yu, Eu^{3+}-activated double perovskite Sr_3MoO_6 phosphors with excellent color purity for high CRI WLEDs and flexible display film, Ceram. Int. 45 (15) (2019) 18604–18613, https://doi.org/10.1016/j.ceramint.2019.06.084.

[17] X. Huang, Q. Sun, B. Devakumar, Preparation, crystal structure, and photoluminescence properties of high-brightness red-emitting $Ca_2LuNbO_6:Eu^{3+}$ double-perovskite phosphors for high-CRI warm-white LEDs, J. Lumin. 225 (2020), 117373, https://doi.org/10.1016/j.jlumin.2020.117373.

[18] S. Wang, B. Devakumar, Q. Sun, J. Liang, L. Sun, X. Huang, Efficient green-emitting $Ca_2GdZr_2Al_3O_{12}:Ce^{3+}$, T^{b3}+ phosphors for near-UV-pumped high-CRI warm-white LEDs, J. Lumin. 220 (2020), 117012, https://doi.org/10.1016/j.jlumin.2019.117012.

[19] Y.R. Parauha, V. Chopra, S.J. Dhoble, Synthesis and luminescence properties of RE3+ (RE = Eu^{3+}, Dy^{3+}) activated $CaSr_2(PO_4)_2$ phosphors for lighting and dosimetric applications, Mater. Res. Bull. 131 (2020), 110971, https://doi.org/10.1016/j.materresbull.2020.110971.

[20] S. Wang, Q. Sun, B. Devakumar, J. Liang, L. Sun, X. Huang, Novel high color-purity Eu^{3+} -activated $Ba_3Lu_4O_9$ red-emitting phosphors with high quantum efficiency and good thermal stability for warm white LEDs, J. Lumin. 209 (2019) 156–162, https://doi.org/10.1016/j.jlumin.2019.01.050.

[21] P. Du, X. Huang, J.S. Yu, Facile synthesis of bifunctional Eu^{3+}-activated $NaBiF_4$ red-emitting nanoparticles for simultaneous white light-emitting diodes and field emission displays, Chem. Eng. J. 337 (2018) 91–100, https://doi.org/10.1016/j.cej.2017.12.063.

[22] X. Huang, H. Guo, B. Li, Eu^{3+}-activated $Na_2Gd(PO_4)(MoO_4)$: A novel high-brightness red-emitting phosphor with high color purity and quantum efficiency for white light-emitting diodes, J. Alloys Compd. 720 (2017) 29–38, https://doi.org/10.1016/j.jallcom.2017.05.251.

[23] T. Sakthivel, G. Annadurai, R. Vijayakumar, X. Huang, Synthesis, luminescence properties and thermal stability of Eu^{3+}-activated $Na_2Y_2B_2O_7$ red phosphors excited by near-UV light for pc-WLEDs, J. Lumin. 205 (2019) 129–135, https://doi.org/10.1016/j.jlumin.2018.09.008.

[24] H. He, R. Fu, Y. Cao, X. Song, Z. Pan, X. Zhao, Q. Xiao, R. Li, $Ce^{3+} \rightarrow Eu^{2+}$ energy transfer mechanism in the $Li_2SrSiO_4:Eu^{2+}$, Ce^{3+} phosphor, Opt. Mater. (Amst) 32 (5) (2010) 632–636, https://doi.org/10.1016/j.optmat.2010.01.009.

[25] X. Huang, W. Zhang, X. Wang, J. Zhang, Optical characteristics and energy transfer between Eu^{3+} and Dy^{3+} in $Na_2CaSiO_4:Dy^{3+}$, Eu^{3+} white-emitting phosphor, J. Alloys Compd. 873 (2021) 159803, https://doi.org/10.1016/j.jallcom.2021.159803.

[26] R.L. Mubiao Xie, Yubin Li, $Na_2CaSiO_4:Eu^{3+}$-deep red-emitting phosphors with intense 5D0-7F4 transition, J. Lumin. 136 (2013) 303–306, https://doi.org/10.1149/2.040301jss.

[27] Y. Shi, Z. Yang, W. Wang, G.e. Zhu, Y. Wang, Novel red phosphors $Na_2CaSiO_4:Eu^{3+}$ for light-emitting diodes, Mater. Res. Bull. 46 (7) (2011) 1148–1150, https://doi.org/10.1016/j.materresbull.2011.03.001.

[28] N. Shaishta, W.U. Khan, S.K.B. Mane, A. Hayat, D.D. Zhou, J. Khan, N. Mehmood, H.K. Inamdar, G. Manjunatha, Red-emitting $CaSc_2O_4:Eu^{3+}$ phosphor for NUV-based warm white LEDs: structural elucidation and Hirshfeld surface analysis, Int. J. Energy Res. 44 (2020) 8328–8339, https://doi.org/10.1002/er.5376.

[29] Y.R. Parauha, S.j., Dhoble, Photoluminescence and electron-vibrational interaction in 5d state of Eu^{2+} ion in $Ca_3Al_2O_6$ down-conversion phosphor, Opt. Laser Technol. 142 (2021), 107191, https://doi.org/10.1016/j.optlastec.2021.107191.

[30] Y.R. Parauha, N.S. Shirbhate, S.J. Dhoble, Color-tunable luminescence by energy transfer mechanism in RE (RE = Eu^{2+}, Tb^{3+})–doped Na_2SrPO_4F phosphors, J. Mater. Sci. Mater. Electron. 33 (2022) 15333–15345, https://doi.org/10.1007/s10854-022-08423-2.

[31] W.N. Wang, W. Widiyastuti, T. Ogi, I.W. Lenggoro, K. Okuyama, Correlations between crystallite/particle size and photoluminescence properties of submicrometer phosphors, Chem. Mater. 19 (2007) 1723–1730. 10.1021/cm062887p.

[32] X. Huang, S. Wang, J. Liang, B. Devakumar, Eu^{3+}-activated Ca_2YTaO_6 double-perovskite compound: A novel highly efficient red-emitting phosphor for near-UV-excited warm w-LEDs, J. Lumin. 226 (2020), 117408, https://doi.org/10.1016/j.jlumin.2020.117408.

[33] Y. Parauha, S.J. Dhoble, Synthesis and luminescence characterization of Eu^{3+} doped $Ca_7Mg_2(PO_4)_6$ phosphor for eco-friendly white LEDs and TL Dosimetric applications, Luminescence. 2 (2020), https://doi.org/10.1002/bio.3900.

[34] G.V. Kanmani, V. Ponnusamy, G. Rajkumar, M.T. Jose, Development of novel $Na_2Mg_3Zn_2Si_{12}O_{30}:Eu^{3+}$ red phosphor for white light emitting diodes, Opt. Mater. (Amst). 96 (2019), 109350, https://doi.org/10.1016/j.optmat.2019.109350.

[35] X. Geng, Y. Xie, Y. Ma, Y. Liu, J. Luo, J. Wang, R. Yu, B. Deng, W. Zhou, Abnormal thermal quenching and application for w-LEDs: Double perovskite $Ca_2InSbO_6:Eu^{3+}$ red-emitting phosphor, J. Alloys Compd. 847 (2020), 156249, https://doi.org/10.1016/j.jallcom.2020.156249.

[36] N. Venkatesh Bharathi, T. Jeyakumaran, S. Ramaswamy, S.S. Jayabalakrishnan, Synthesis and characterization of a Eu^{3+}-activated $Ba_{2-x}V_2O_7:xEu^{3+}$ phosphor using a hydrothermal method: a potential material for near-UV-WLED applications, Luminescence. 36 (2021) 849–859, https://doi.org/10.1002/bio.4031.

[37] D.L. Shruthi, A. Jagannatha Reddy, G.N. Anil Kumar, Structural, Judd-Ofelt, photoluminescence properties of Eu^{3+} activated $SrWO_4$ phosphors: Electronic, vibrational, elastic properties from ab initio study, Opt. Mater. (Amst). 118 (2021), 111243, https://doi.org/10.1016/j.optmat.2021.111243.

[38] G. Yuan, R. Cui, J. Zhang, X. Zhang, X. Qi, C. Deng, Photoluminescence evolution and high thermal stability of orange red-emitting $Ba_{3-x}Sr_xZnNb_2O_9:Eu^{3+}$ phosphors, J. Solid State Chem. 303 (2021) 122447, https://doi.org/10.1016/j.jssc.2021.122447.